The binding of Varp to VAMP7 traps VAMP7 in a closed, fusogenically inactive conformation.

Ingmar B. Schäfer[1$], Geoffrey G. Hesketh[2], Nicholas A. Bright[2], Sally R. Gray[2], Paul R. Pryor[2†], Philip R Evans[1], J. Paul Luzio[2]*and David J. Owen[2]*

[1]Medical Research Council Laboratory of Molecular Biology, Hills Road , Cambridge CB2 0QH, UK

[2]Cambridge Institute for Medical Research, University of Cambridge, Addenbrooke's Hospital, Hills Road, Cambridge. CB2 0XY, UK

[$]Current address: Max Planck Institute of Biochemistry, Department of Structural Cell Biology, Am Klopferspitz 18, D-82152 Martinsried, Germany

[†]Current address: Department of Biology (Area 9), University of York, York Y010 5YW, UK

Supplementary Information

Supplementary Figure 1: The full length cytoplasmic domain of VAMP7 but not its longin domain alone binds to Varp

a

Clone number	Start-end of nucleotide sequence	Start-end of protein sequence
1	1805-2584	551-810
2	1805-2604	551-816
3	1805-2664	554-837
4	1814-2681	554-842
5	2080-2829	642-891
6	2080-2882	642-909
7	2080-2891	642-912
8	2080-2892	642-912
9	2080-2985	642-943
10	2082-2924	643-923
11	2167-2348	671-731

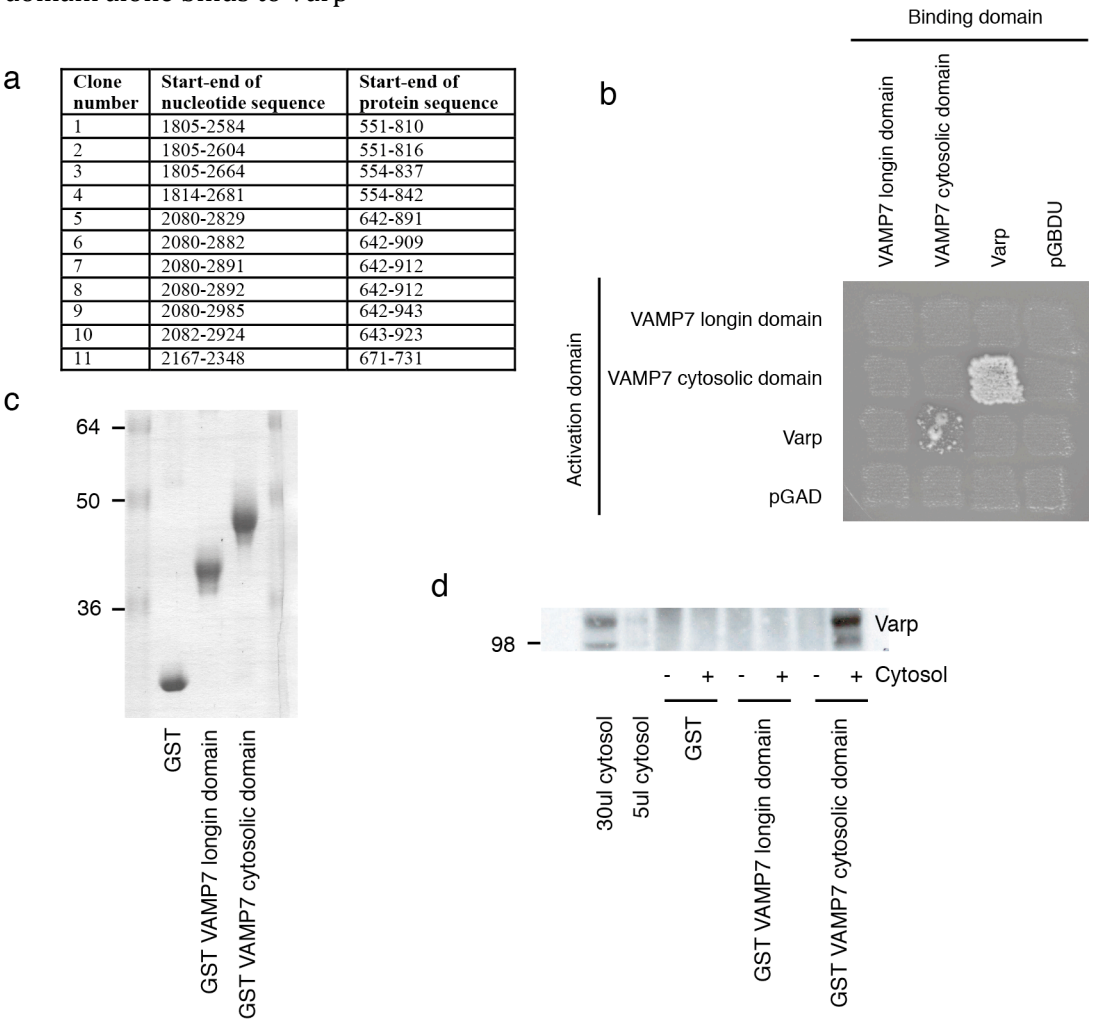

a Domain boundaries of VAMP7-interacting Varp clones identified in Y2H screen of K562 erythroleukemia cDNA library with VAMP7CD as bait (Nucleotide sequence accession no. NM_032139)

b Grid of yeast-2-hybrid interactions between VAMP7 cytosolic domain, VAMP7 longin domain and Varp when expressed from both DNA binding domain (pGBDU) and activation domain (pGAD) plasmids carried out as in [1]. An interaction as assessed by growth of diploid strains containing the indicated plasmids on medium lacking adenine was detected only between the full length cytosolic domain of VAMP7 and Varp and not between the VAMP7 longin domain and Varp.

c Coomassie staining of SDSPAGE showing GSTVAMP7 cytosolic domain, GSTVAMP7 longin domain and GST alone used in pull downs from human MNT-1 melanoma cells cytosol in **d**.

d Western blot following 'GST pull downs' from MNT-1 cytosol developed using an in-house rabbit polyclonal antibody against Varp shows that GSTVAMP7 cytosolic domain but not GSTVAMP7 longin domain or GST alone could bind to endogenous Varp

Supplementary Figure 2: Binding of Varp to VAMP7

a

run number	stoichiometry of binding sites (N)	K_D [μM]	ΔH [cal mol^{-1}]	ΔS [cal mol^{-1} °C^{-1}]
1	1.03 ± 0.007	2.67 ± 0.09	-6077 ± 55	3.6
2	1.01 ± 0.006	3.21 ± 0.08	-6356 ± 9	2.2
3	1.03 ± 0.007	1.71 ± 0.08	-8715 ± 76	-5.0
4	1.01 ± 0.01	1.72 ± 0.13	-9501 ± 146	-7.9

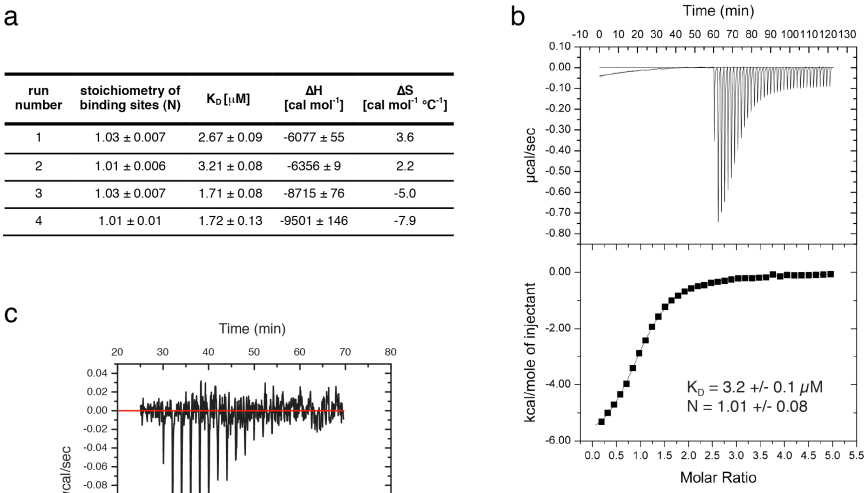

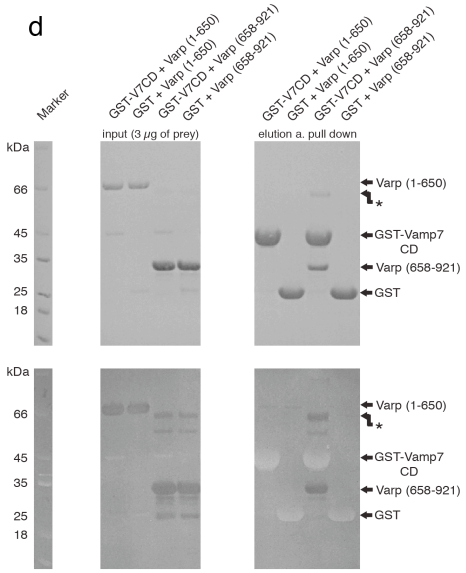

a Individual K_D values from 4 ITC runs of Varp 658-921 binding to full length VAMP7 cytosolic domain. The average strength of the interaction is 2.3 ±0.6 μM with an average N value of 1.02 and the interaction in enthalpically driven.

b Representative ITC experiment for the binding of Varp 658-921 binding to full length VAMP7 cytosolic domain (run 2 in **a**)

c That no additional VAMP7 binding site in Varp exists other than that described here is also supported by ITC that demonstrates despite the tendency of full length Varp to precipitate on stirring in an ITC machine, the K_Ds for the binding of full length Varp and residues 658-921 of Varp to full length VAMP7 cytosolic domain are similar: 3±1μM and 2.3±0.6μM respectively

d Coomassie staining of SDS PAGE (top panels) and anti-His tag Western blot (bottom panels) of a 'GST pull downs' using the GSTVAMP7 cytosolic domain as bait and Varp (1-650)-H10 and Varp (658-921)H10 as prey. The left hand panels show 1% (~3mg) of the starting materials while the right hand panels show the results of the experiments. These show that the N-terminal portion of Varp (residues 1-650) does not bind to VAMP7 cytosolic domain, ie it does not contribute to the binding of VAMP7 by Varp.

Supplementary figure 3. Localisation of Varp in cells and the lack of effect of Varp depletion

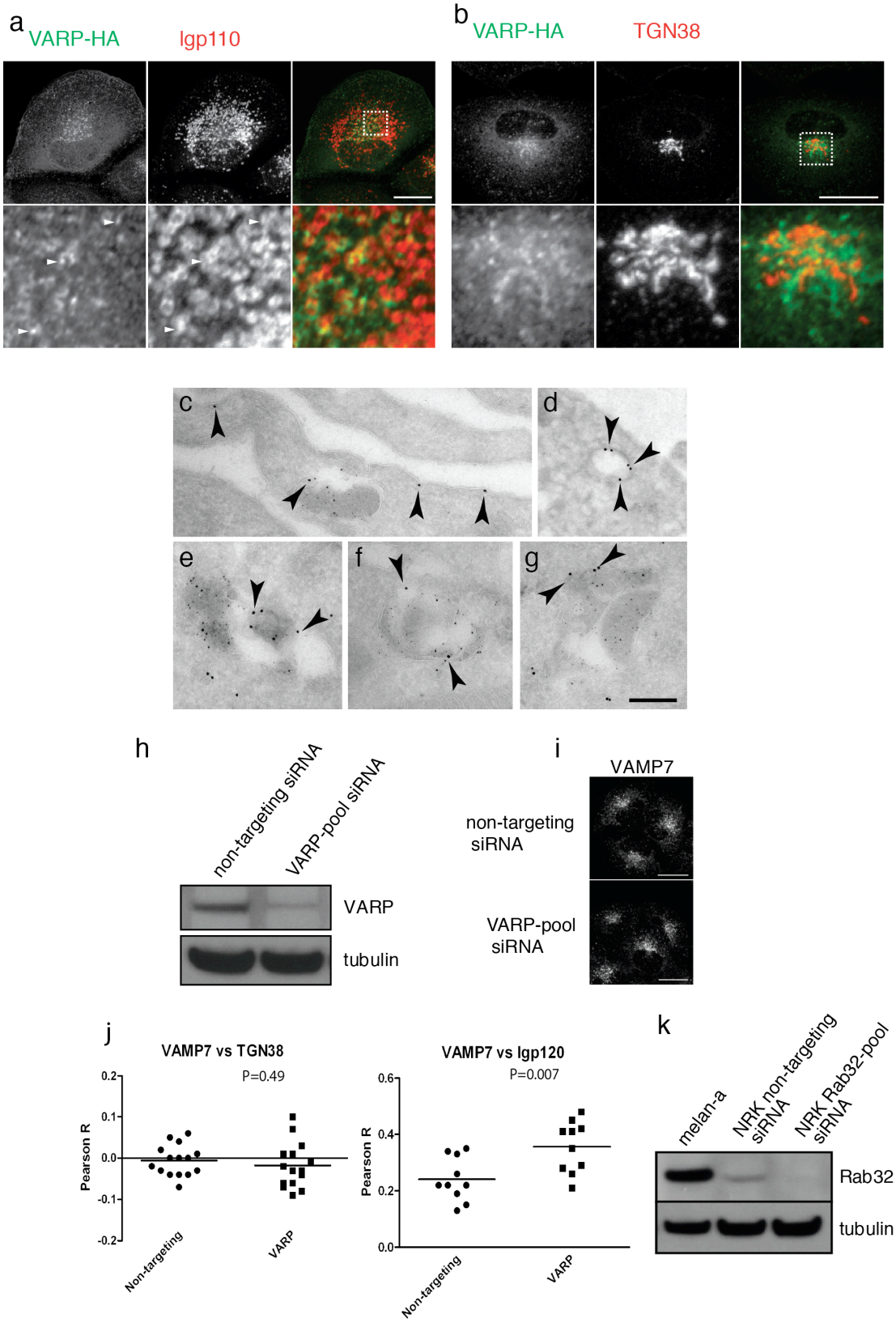

a and **b** Representative images of VARP-HA and (**a**) endogenous lgp110 (otherwise known as LAMP2)or (**b**) endogenous TGN38 were imaged by immuno-fluorescent confocal microscopy in NRK cells stably expressing VARP-HA. Bottom panels are zoomed in images of the boxed regions, and arrowheads indicate representative structures positive for both markers. Partial co-localisation is seen with lgp110 and virtually no colocalisation with TGN38. Scale bars = 20μm

c to **g** NRK cells stably expressing Varp-HA, into which Dextran-Texas Red had been endocytosed for 4h followed by a 20h chase to label lysosomes, were prepared for immunogold electron microscopy and labeled with antibodies to Texas Red (5nm gold), lgp110 (10nm gold) or the HA tag (15nm gold). Anti-HA immunoreactivity (representative examples indicated by large arrowheads) was associated with the plasma membrane (**c**), early endosomes adjacent to the plasma membrane but devoid of Texas Red or lgp110 immunoreactivity (**d**) or dense core lysosomes co-immunolabelled with anti-Texas Red and anti-lgp110 on ultrathin cryosections (**e-g**). Scale bar = 200 nm.

h-j Effect of si-RNA knockdown of Varp on VAMP7 localisation. NRK cells treated for 5 days with a pool of 4 siRNA oligos against Varp (VARP) or with a non-targeting control oligo (NT). Efficiency of Varp depletion was quantified as 75% by Western blotting (**h**). Cells were immunofluorescently stained for endogenous VAMP7 (rabbit polyclonal) and either TGN38 (mouse monoclonal 2F7.1) or lgp120 (also known as LAMP1) (mouse monoclonal LY1C6, Assay Designs) (**i**). Single confocal sections were obtained for 15 (TGN38) or 10 (lgp120) independent fields (>5 cells/field). **j** The degree of colocalization (expressed as a Pearson coefficient R) was determined for each field using the Carl Zeiss Zen image analysis software. Pearson R coefficients with and without Varp depletion were graphed using GraphPad Prism software. For VAMP7 vs TGN38 the mean Pearson R coefficients±SEM were -0.01 ± 0.01 (15) after treatment with non-targeting siRNA and -0.02 ± 0.01 (15) after treatment with siRNA against Varp. The mean Pearson R coefficient for VAMP7 vs lgp120 were 0.24 ± 0.02 (10), for non-targeting siRNA and 0.38±0.03 (10) for siRNA against Varp. The differences in the means were statistically analyzed using an unpaired two-tailed t-test (VAMP7 vs TGN38, P=0.49; VAMP7 vs lpg120, P=0.007). SiRNA depletion of Varp has no effect on VAMP7 vs TGN38 colocalisation whereas there was a subtle but reproducible increase in the colocalisation of VAMP7 vs lgp120 (increase in Pearson R coefficients from 0.22 to 0.38) suggesting that there had been an increase in the fusion of earlier and later compartments of the endocytic pathway

k NRK cells were treated with either a non-targeting siRNA control oligo-nucletotides (middle lane) or a pool of 4 individual siRNA oligo-nucleotides targeting Rab32 (right lane) were Western blotted using an antibody against Rab32. Loss of the Western blot signal upon Rab32 depletion demonstrates Rab32 protein expression in NRK cells. Melan-a mouse melanocytes were used as a positive control for Rab32 staining (left lane). Tubulin staining was used as a loading control.

Supplementary figure 4: X-ray structure determination of Varp658-921–VAMP7 CD complex

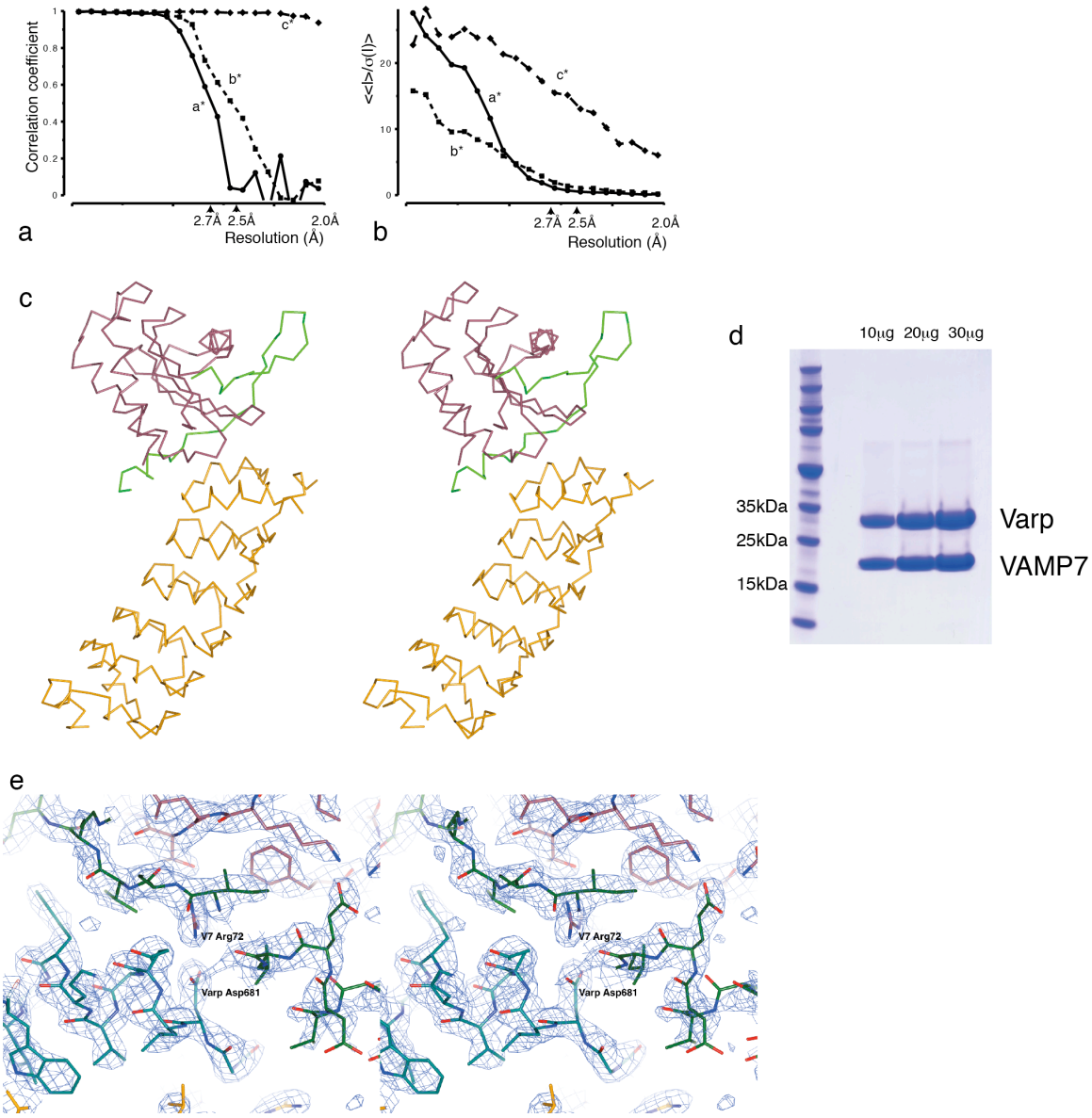

a and **b** plots showing the anisotropic resolution dependence of the native data, analysed by resolution in cones of semi-angle 20° around the a*, b* and c* axes, showing good resolution along c*, but worse resolution along a* and c* (to about 2.7Å and 2.5Å respectively, see table 1). **a** correlation coefficient between two random halves of the data **b** average signal to noise ratio <<I>/σ(<I>)>

c Stereo view of the Cα trace, yellow Varp, purple Vamp7 longin domain, green Vamp7 SNARE motif. **d** Coomassie blue stained SDSPAGE of the Varp(658-921)–VAMP7 complex eluting from the final gel filtration step and used for crystallisation showing a 1:1 stoichiometry. **e** Stereo view of part of the experimental phased electron density

Supplementary figure 5: Comparison of the Varp–VAMP7 interaction with other ankyrin repeat mediated protein:protein interactions

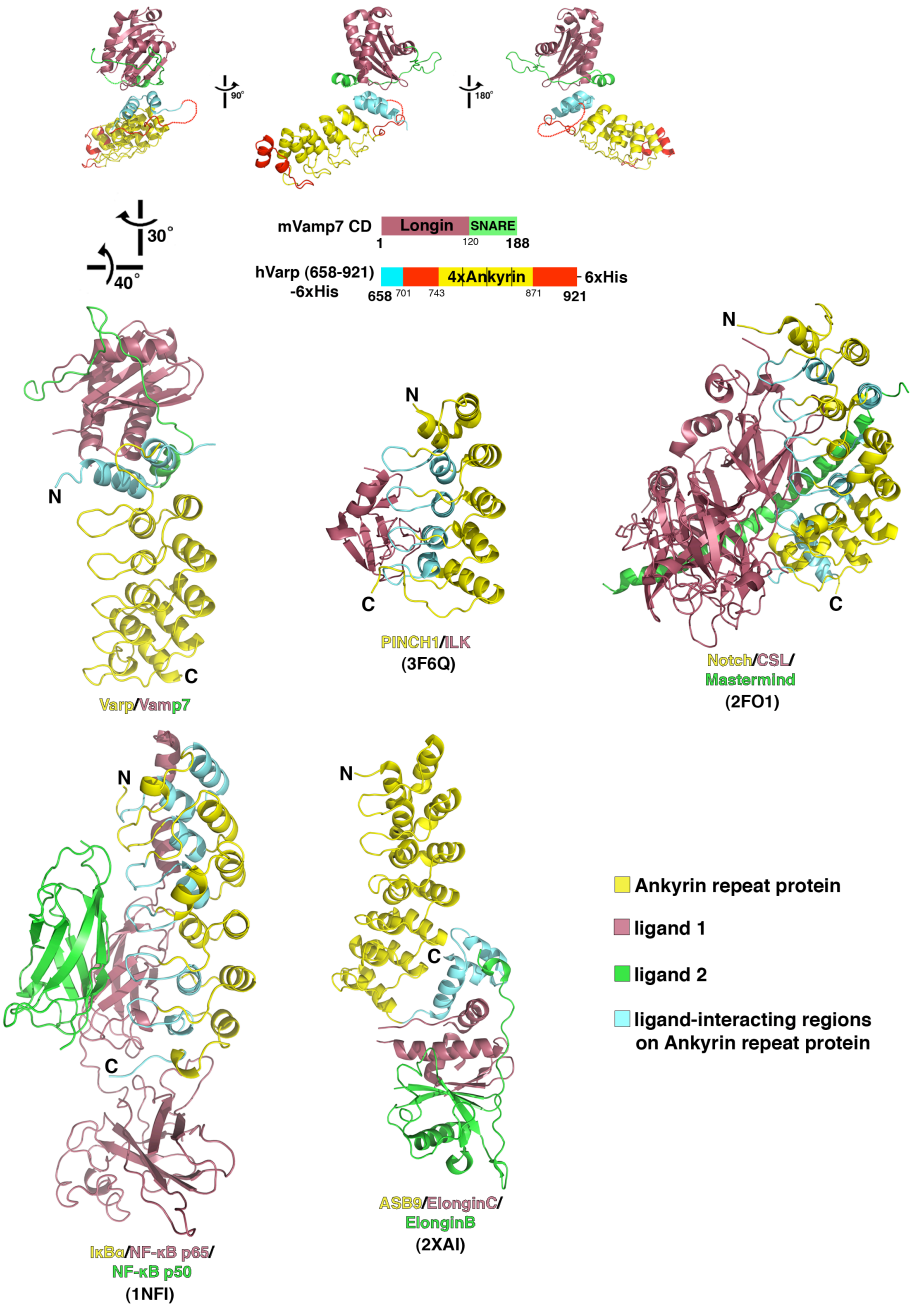

The parts of the Ankyrin repeats that mediate the interaction with the ligand(s) are in all structures displayed in cyan as the ligand binding Ankyrin repeat of Varp. The PDB codes of each of the shown structures are: 3F6Q,[2]; 1NFI,[3]; 2FO1[4], and 2XAI (to be published). A fifth not-shown structure of the Osteoclast stimulating factor with the accession code 3EHR [5] consists of one polypeptide chain containing a SH3 domain followed by an Ankyrin repeat stack. In this case the SH3 domain sits on top of the Ankyrin repeat stack in a manner similar to that of the Varp–VAMP7 complex here with the important difference that both SH3 domain and Ankyrin repeat are part of the same protein.

Supplementary Figure 6: Varp and VAMP7 sequences

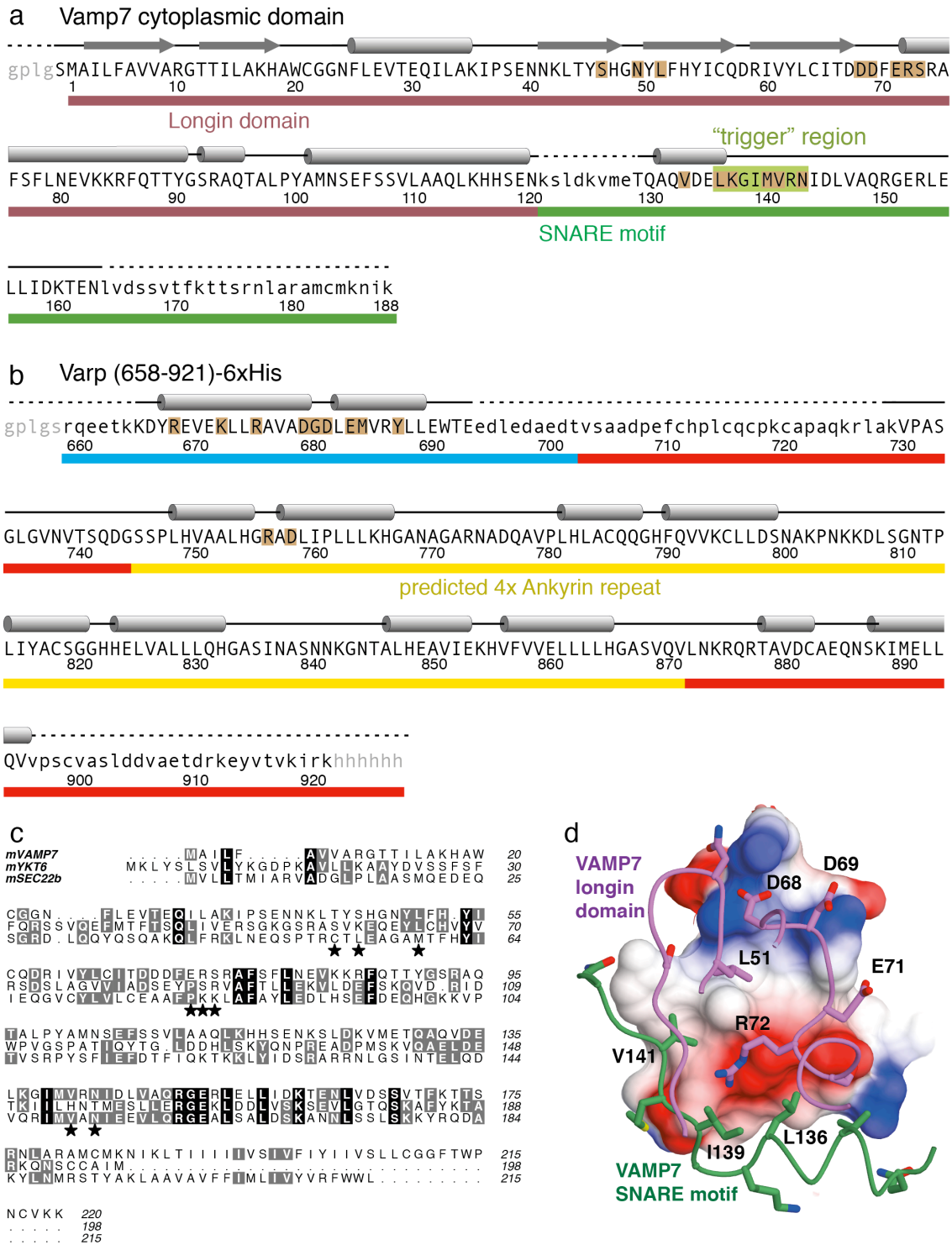

a, b Primary sequences with secondary structure and domains indicated (arrows for β–sheet strands and cylinders for α-helices) of the portions of Varp and VAMP7 crystallised

as a complex. Domains are coloured as in Figure 1d. Residues involved in the Varp–Vamp7 interaction are shaded brown. The SNARE "trigger" region in Vamp7 is shaded green.
c Sequence alignment of VAMP7, Ykt6 and Sec22b. Conserved residues are shaded and those involved in the interaction of VAMP7 with Varp are marked with stars. Most of the residues involved in the interaction between VAMP7 and Varp are not conserved in Ykt6 and Sec22b explaining why these longin domain containing SNAREs show no binding to Varp (shown in Figure 1)
d Interface between Varp (shown as a molecular surface coloured by electrostatic potential (blue positive, red negative)) and VAMP7LD (purple) and VAMP7 SNARE motif (green), showing that R72 (VAMP7LD) interacts with a complementary patch of negative charge. This charged interaction is surrounded by hydrophobic residues V133, L136, I139, M140 and V141 from the SNARE motif, protecting it from solvent.

Supplementary figure 7: Time resolved analysis of the *in vitro* reconstitution of the syntaxin7–syntaxin8–Vti1B–VAMP7 SNARE complex in the presence of Varp, short time course

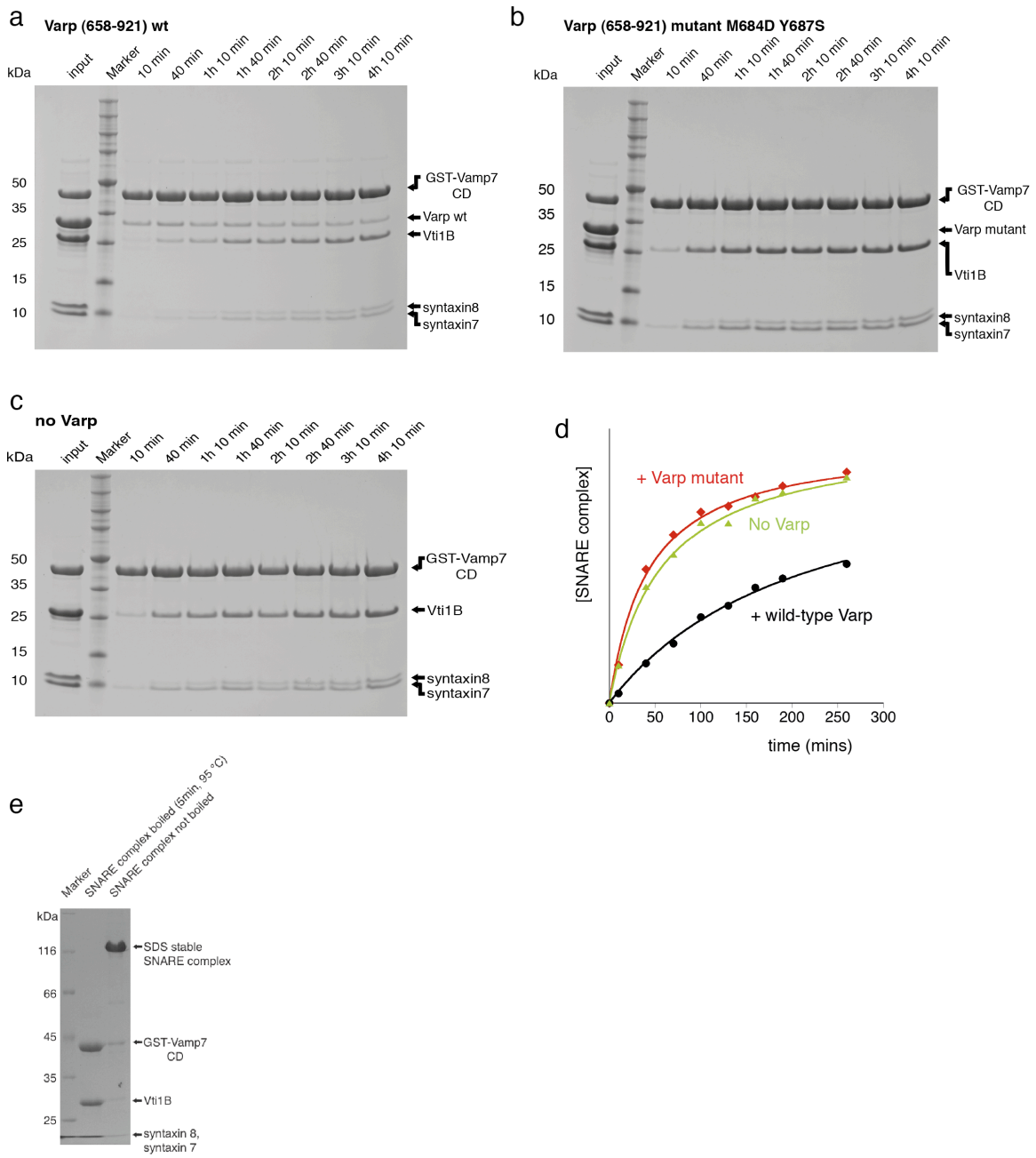

To analyse the kinetic inhibitory effect of Varp on the formation of VAMP7 containing SNARE complexes the syntaxin7–syntaxin8–Vti1b–VAMP7 SNARE complex was reconstituted on GSTVAMP7 in the absence and the presence of Varp 658-921 and in the presence of the non-VAMP7 binding mutant form of Varp 658-921, M684D Y687S. Syntaxin7, syntaxin8, Vti1b and GSTVAMP7 were mixed in the molar ratios 4:4:4:1 and Varp 658-921 forms added in the molar ratio 4:1 to GSTVAMP7. At time points 0min, 30min, 1h, 1h 30min, 2h, 2h 30min, 3h and 4h samples were taken and incubated for 10 min with GSH-sepharose. The SNARE complex reconstitution reaction was consequently stopped by washing off excess free SNAREs and Varp at time points 10min, 40min, 1h 10min, 1h 40min, 2h 10min, 2h 40min, 3h 10min and 4h 10min.

The samples were analysed on Coomassie stained SDS PAGE gels: panel **a** "Varp wt" shows the SDS PAGE gel of the SNARE complex reconstitution reaction in the presence of Varp 658-921 wt, panel **b** "Varp M684D Y687S" the SDS PAGE gel of the reconstitution reaction in the presence of Varp 658-921 M684D Y687S and panel **c** "no Varp" the SNARE complex reconstitution reaction in the absence of Varp. Panel **d** shows the quantification of the reconstitution reactions **a-c**. The relative amount of SNARE complex (vertical axis) at each of time point (horizontal axis) was measured from the Vti1B band. The presence of Varp (black) slows the formation of the SNARE complex compared to the reaction in the absence of Varp (green) and in the presence of the non-VAMP7 binding mutant version of Varp M684D Y687S (red). Curves were fitted using a second-order rate equation, giving rates relative to wt Varp of 3.9 in the absence of Varp and 5.1 for the Varp mutant, ie the Varp mutant has essentially no effect on SNARE complex formation.
e Coomassie blue stained SDSPAGE showing that the reconstituted SNARE complex is SDS-stable: in the presence of SDS without boiling, the complex runs as a single band (right hand lane), but separates into its constituents on boiling for 5 minutes in SDS containing sample buffer (middle lane) and only forms when all four SNAREs are present [6-8]. Complexes involving VAMP8 show the same SDS stability that can be overcome by 5 minutes boiling in SDS sample buffer ([6] and data not shown)

Supplementary figure 8: Time resolved analysis of the influence of Varp and the VAMP7 longin domain on the *in vitro* reconstitution of the syntaxin7–syntaxin8–Vti1B–VAMP7 SNARE complex, long time course

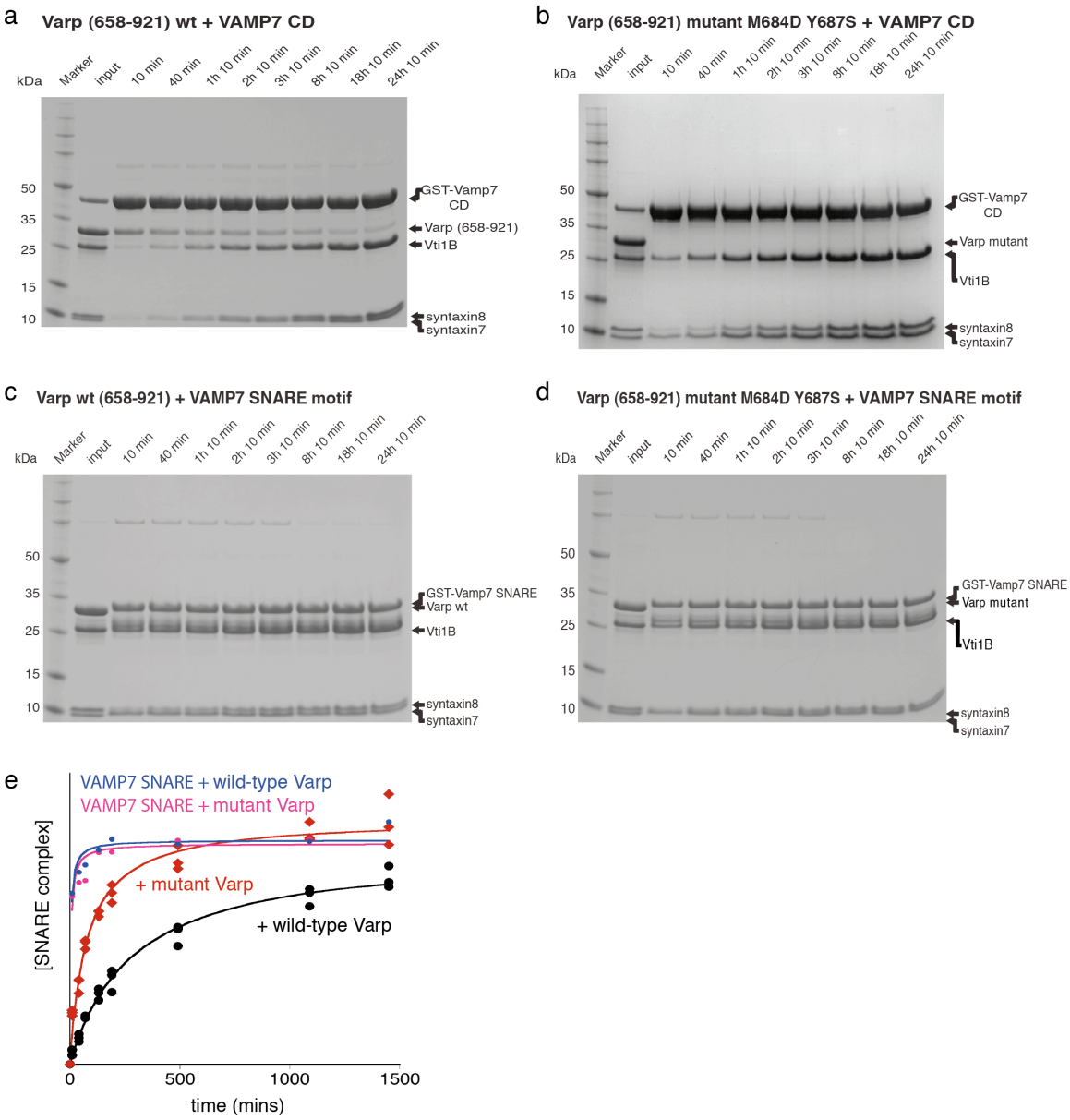

To analyse the kinetic effect of Varp and the VAMP7 longin domain on the formation of Vamp7 containing SNARE complexes the syntaxin7–syntaxin8–Vti1b–VAMP7 SNARE complex was reconstituted on GSTVAMP7 cytosolic domain (CD) or GSTVAMP7 SNARE motif in the presence of Varp 658-921 and in the presence of the non-VAMP7 binding mutant form of Varp 658-921, M684D Y687S.

SNARE complexes were reconstituted in the presence of the Varp forms as described in the legend of Supp. Figure 7 with the difference that the samples were taken at time points 0min, 30min, 1h, 2h, 3h, 8h, 18h and 24h and reactions consequently stopped at time points 10min, 1h 10min, 2h 10min, 3h 10min, 4h 10min, 8h 10min, 18h 10min and 24h 10min. The experiments with VAMP7 CD were carried out three times.

Panel **a** “Varp wt” shows one of the three SDS PAGE gels of the SNARE complex reconstitution reactions in the presence of Varp 658-921 wt, panel **b** “Varp M684D Y687S” one of the three SDS PAGE gels of the reconstitution reactions in the presence of Varp 658-921 M684D Y687S, panel **c** “GSTV7 SNARE + Varp wt” the SNARE complex reconstitution reaction on GSTVAMP7 SNARE motif in the presence of Varp 658-921 wt and panel **d** “GSTV7 SNARE + Varp M684D Y687S” the SNARE complex reconstitution reaction on GSTVAMP7 SNARE motif in the presence of Varp 658-921 M684D Y687S. In Panel **e** (same as fig 6d) the quantification of the syntaxin7 and 8 bands of the experiments is plotted against the reaction time. Note that the Vti1b band could not used in this case to quantitate the reaction product as it obscured by the GSTVAMP7 SNARE motif bands in case c and d. As in supplementary figure 7, each curve was fitted to a second-order rate equation. In the case of the experiments with VAMP7 CD (sample gels in panels a and b), the points from the three different runs were treated as separate observations. Fitted rates relative to wt Varp were 3.3 for the Varp mutant, and 71 and 63 for the much faster reactions with the GSTVAMP7 SNARE motif. The SNARE complex formation is fastest in the absence of the longin domain, intermediate in its presence without Varp (Fig S7) and slowest in the presence of both the longin domain and Varp.

Supplementary Note

DNA Constructs

A silent mutant of the IMAGE-clone IMAGE 6067580 in which the *Hind*III site had been removed by PCR mediated mutagenesis was used as template for all VARP constructs described here and the. The Rab38 clone (Addgene plasmid 15669) was created in the laboratory of William Pavan and the mRFP-Rab7 plasmid (Addgene plasmid 14436) was created in the laboratory of Ari Helenius and were purchased from Addgene. Constructs used in this study included pGEX-4T1 and pGEX-6P1 VAMP7 (1 to 188), pGEX-6P1 VAMP7 (1 to 188) (R72A), pGEX-6P1 VAMP7 (1 to 188) (D69A, E71F, S73D), pGEX-4T1 VAMP7 (1 to 120), pGEX-4T1 VAMP7 (120 to 188), pGEX-4T1 VAMP7 (1 to 180), pGEX-4T1 VAMP7 (1 to 170), pGEX-4T1 VAMP7 (1 to 160), pGEX-4T1 VAMP7 (1 to 150), pGEX-4T1 VAMP7 (1 to 140), pGEX-4T1 VAMP7 (1 to 130), pMW VARP (1-1050)-His_{10}, pMW VARP (1-650)-His_{10}, pGEX-6P1 VARP (653-962)-His_6, pGEX-6P1 VARP (658-1013)-His_6, pGEX-6P1 VARP (658-921)-His_6, pGEX-6P1 VARP (658-921)-His_6 (M684S, Y687D), pGEX-6P1 VARP (658-921)-His_6 (D679A, D681A), pGEX-6P1 VARP (451-921)-His_6, pGEX-6P1 VARP (718-1050)-His_6, pGEX-6P1 VARP (718-921)-His_6, pGEX-4T1 rab38, pGEX-4T1 and pGEX-6P1 rab38 (Q69L), pGEX-4T1 and pGEX-6P1 rab38 (T23N), pGEX-6P1 rab32 (Q85L), pGEX-6P1 rab32 (T39N), pGEX-4T2 Vti1B (117-206), pMW His_6-Vti1B (1-206), pMW His_6-syntaxin7 (169-237), pMW His_6-syntaxin8 (149-213), pMW His_6-Vamp8 (1-76), pET32a Vamp8 (1-76), pGEX-4T3 Ykt6 (1 to 196), pGEX-4T3 Sec22b (1 to 191) and pLIXN-Varp (1-1050)-2xHA.

For Y2H analysis DNA constructs included pGAD VAMP7(1-188) pGAD VAMP7 (1-120) pGAD Varp(1-1050) pGBDU VAMP7(1-188) pGBDU VAMP7 (1-120) and pGBDU Varp (1-1050). Interactions were assessed as in [1]

Antibodies

The antibodies used in this study were: anti-HA mouse monoclonal (clone 16B12, Covance, Cat#MMS-101R), anti-Varp rabbit polyclonal (4038, see method below), anti-VAMP7 rabbit polyclonal (gift of Andrew Peden), anti-dsRed rabbit polyclonal (Clontech, Cat#632496), anti-rat lgp110 rabbit polyclonal (580) and anti-rat TGN38 rabbit polyclonal [9], anti-rat LAMP1 mouse monoclonal (clone LY1C6, Enzo Life Sciences) anti-α-tubulin mouse monoclonal (clone DM1A, Sigma, Cat#T6199), anti-Texas Red (Molecular Probes [Invitrogen]), anti-Rab32 rabbit polyclonal (gift of Tina Wassmeir and Miguel Seabra) and rabbit anti-mouse immunoglobulin (Sigma). A rabbit anti-Varp polyclonal antibody was raised against human Varp (658-921) by Cambridge Research Biochemicals. Antibody was affinity purified from sera using Varp (658-921) conjugated to Affigel affinity matrix (BioRad).

Limited proteolysis of hVARP (1-1050)-His_{10}

Varp (1-1050)-His_{10} was mixed in a mass ratio of 5000:1 with Chymotrypsin (10 mg ml^{-1} in milliQ water, freshly weighed from dry powder) and incubated at 23 °C. 20 µl samples of the reaction were taken after 0, 5, 10, 15, 20, 30, 45 and 60 minutes, the proteolytic reaction was stopped by the addition of 2 µl of the protease inhibitor stock (1 complete, EDTA free protease inhibitor tablet (*Roche*) in 100 µl of miliQ water) and boiling the samples in SDS-loading buffer. Samples were then analysed by Western Blotting with HisProbe-HRP conjugate (*Thermo Scientific*) allowing detection of Varp fragments with intact C-terminii or by transfer onto PVDF membrane followed by N-terminal sequencing of any significant bands. Domain analysis and prediction of foldedness was carried out using globplot2 [10] and the secondary structure consensus prediction of the NPS@ server [11] (see Figure 1).

ITC and pull downs

For pull downs 50 μg of the GST-tagged bait was incubated with 300 μg of the untagged prey protein and 60 μl of a 50 % (v/v) GSH-Sepharose-slurry (*GE Healthcare*) for 1 h at 4 °C on a roller incubator (total volume 250 μl). In the case of the Vamp7CD-His_{12}–Varp(451-650)-His_6 pull down with GST-Rab38 the two prey proteins were added to the reaction in a 1:1 molar ratio in the amounts indicated in figure 7 A. The beads were washed 4 to 5 times with 1 ml of pull-down buffer (Varp–VAMP7: 500 mM NaCl, 20 mM HEPES pH 7.4, 10 mM DTT, 1 mM EDTA; Varp–Vamp7–Rab38: 500 mM NaCl, 20 mM HEPES pH 7.4, 10 mM DTT, 5 mM $MgCl_2$, 100 μM GDP or GTPγS supplemented with 1 % (w/v) NP40).

The proteins were eluted off the beads using 50 μl of a solution of 30 mM reduced GSH in the pull-down buffer. The samples were analysed on SDS-PAGE and/or Western Blots, which were probed with the HisProbe-HRP conjugate (*Thermo Scientific*). As negative control either GST alone or a protein that was known not to interact with the prey was used as bait (for example the GDP-looked mutant of Rab38, GST-Rab38 T23N).

For ITC measurements all proteins were gel filtered into the appropriate ITC buffer (buffer: 200 mM NaCl, 50 mM HEPES pH 7.4, 10 mM β-mercaptoethanol) prior to the measurements. All measurements using Varp 658-921 were performed at 4 °C with a VP-ITC isothermal titration calorimeter (*MicroCal*) and those using full length Varp were carried out on an ITC200 (*Microcal*). For the measurements of the binding of VARP to VAMP7 300 μM of the respective VAMP7 construct was loaded into the syringe and 20 μM of the wild type or mutant VARP (658-921)-His_6 was loaded into the cell. To determine the K_D of a binding reaction the mean of four independent ITC measurements that showed clear signs of saturation of the binding by the end of the run were used and the SD calculated (see Supp figure 2).

SNARE complex inhibition assays

The syntaxin7–syntaxin8–Vti1b–VAMP7 SNARE complex was reconstituted from purified recombinant SNARE proteins. This final SNARE complex was estimated as having a stoichiometry of 1:1:1:1, only formed when all four components were present (data not shown), was SDS stable and required boiling for 5 minutes in SDS sample buffer to dissociate it into its individual components (Supplementary figure 7 and described in [6-8]). In each case the molar ratio of the respective GST-tagged bait protein to the prey proteins was 1:4 (concentration of used proteins: GST-VAMP7 (1-188), GST-Vti1B (117-206), Syntaxin7 (169-237)-His_6, Syntaxin8 (149-213)-His_6, Vti1b (1-206)-His_6 all 20 mg ml^{-1} and VAMP7 (1-188) 10 mg ml^{-1}). To assess the influence of VARP on SNARE complex formation different amounts of Varp (658-921)-His_6, Varp (658-921)-His_6 and VAMP7 (1-188) CD complex or Varp (658-921)-His_6 M684D Y687S (concentration of stock solutions: 20 mg ml^{-1}, 10 mg ml^{-1} and 12.2 mg ml^{-1} respectively) were added to the reconstitution reactions.

In case of the assay using GST-VAMP7 as bait shown in figure 6, the SNARE complex in absence of VARP was reconstituted in the reaction labelled 'V7 CD'. The reaction 'M684D Y687S' of the same assay used GST-VAMP7 and Varp (658-921)-His_6 M684D Y687S in a molar ratio of 1:1 as input. Reactions prepared identically to 'V7 CD' were titrated with increasing amounts of free wt Varp (658-921)-His_6 at the molar rations of GST-VAMP7: Varp of 1:1, 1:2, 1:4, 1:8, 1:16 and 1:32 were labelled '+1x Varp', '+2x Varp', '+4x Varp', '+8x Varp', '+16x Varp ' and '+32x Varp ' respectively on figure 6.

For the assay using GST-Vti1B as bait VAMP7 alone, VAMP7 and Varp (658-921)-His_6 M684D Y687S in a 1:1 molar ratio or preformed VAMP7: Varp (658-921)-His_6 complex was used as input in the reactions labelled 'V7 CD', 'M684D,Y687S' and 'V7 + Varp. To

analyse the concentration dependency of the influence of Varp on SNARE complex formation additional, free Varp (658-921)-His_6 was added to reactions containing VAMP7: Varp (658-921)-His_6 complex (set up in the same way as described for 'V7 + Varp'). Reactions labelled '+1x Varp excess', '+3x Varp excess', '+5x Varp excess', '+7x Varp excess', '+9x Varp excess' therefore contain a final molar ratio of VAMP7 to Varp of 1:2 (1x Varp in VAMP7:Varp complex and 1x free Varp), 1:4 (1x Varp in VAMP7: Varp complex and 3x free Varp), 1:6 (1x Varp in VAMP7: Varp complex and 5x free Varp), 1:8 (1x Varp in VAMP7: Varp complex and 7x free Varp) and 1:10 (1x Varp in VAMP7: Varp complex and 9x free Varp) respectively.

Once set up the reactions were incubated at 4 °C with agitation for 0.5 h or 1.5 h. After this step GSH-Sepharose pull-downs of the reconstitution reactions were performed. 55 µl of a 50 % (v/v) slurry of Glutathione-sepharose was added to each reaction and the samples incubated for 1 h at 4 °C. The beads were subsequently washed 5 times with 1 ml of the reconstitution buffer (500 mM NaCl, 20 mM HEPES pH 7.4, 10 mM DTT, 1 mM EDTA) supplemented with 1 % (w/v) NP40. After this step the bound proteins were eluted by supplementing each sample with 50 µl of elution buffer (500 mM NaCl, 20 mM HEPES pH 7.4, 10 mM DTT, 1 mM EDTA, 30 mM reduced Glutathione) and incubating these reactions for 5 minutes. The samples prepared in this way were analysed by SDS-PAGE and the relevant protein bands of the gel densitometrically quantified using the program *ImageJ*. The integrated peak areas of each gel band of interest were normalised by division with the area of the bait protein band in the particular reaction and this value expressed as ratio of the normalised band area in the absence of Varp (molar ratio of Varp /VAMP7 = 0, lane 'V7 CD') for the syntaxin7, 8, and Vti1b bands in figure 6**b** and for the VAMP7 CD band in figure 6**c**. In the case of the quantification of the VARP (658-921)-His_6 bands in figure 6**b**, the measurements were, after normalization, expressed as a ratio of the normalised band area in the presence of the maximal amount of VARP (molar ratio Varp /VAMP7 = 32, lane '+32x Varp' in figure 6**b**).

For the analysis of the time dependence of the effect of Varp on the formation of the syntaxin7–syntaxin8–Vti1B–VAMP7 assays similar to those one described for GSTVAMP7 was prepared. Three SNARE complex reconstitution reactions, one in the presence of Varp (658-921)-His_6 wt (top panel "Varp wt" Supp. Figure 7**a**), one in the presence of Varp (658-921)-His_6 M684D Y687S (panel "Varp M684D Y687S" Supp. Figure 7**b**) and one in the absence of Varp (panel "no Varp" Supp. Figure 7**c**) were set up. In the case of the experiments shown in Supp. Figure 8 8 independent reactions were prepared: three using GSTVAMP7 CD and Varp (658-921)-His_6 wt (one representative one labelled "Varp wt" shown in Supp. Figure 8**a**), three using GSTVAMP7 CD and Varp (658-921)-His_6 M684D Y687S (one representative one labelled "Varp M684D Y687S" shown Supp. Figure 8**b**), one using GSTVAMP7 SNARE motif and Varp (658-921)-His_6 wt (labelled "GSTV7 SNARE + Varp wt" shown in Supp. Figure 8**c**) and one using GSTVAMP7 SNARE motif and Varp (658-921)-His_6 M684D Y687S (labelled "GSTV7 SNARE + Varp M684D Y687S" shown in Supp. Figure 8**d**). The SNARE proteins were mixed in molar ratios of 4:4:4:1 (syntaxin7:syntaxin8:Vti1B: GSTVAMP7) and Varp forms added if required in a molar ratio of 1:4 GSTVAMP7:Varp. The reactions were subsequently incubated at 4 °C under agitation. At time points 0min, 30min, 1h, 1h 30min, 2h, 2h 30min, 3h and 4h for the assays described in Supp. Figure 7 and at time points 0min, 30min, 1h, 2h, 3h, 8h, 18h and 24h in case of the assays described in Figure 6 and Supp. Figure 8 103 µl of each reaction were removed and supplemented with 55 µl of a 50 % (v/v) slurry of Glutathione-sepharose. The samples were incubated at 4 °C and the reconstitution reaction stopped by washing the beads 5 times with 1ml of reconstitution buffer (stop of reconstitution reactions consequently at time points 10min, 40min, 1h 10min, 1h 40min, 2h 10min, 2h 40min, 3h 10min and 4h 10min in case of Supp. Figure 7 and 10min, 40min, 1h 10min, 2h 10 min, 3h 10min, 8h 10min, 18h 10min and

24h10min for those experiments shown in Figure 6 and Supp Figure 8). After this step the bound proteins were eluted by supplementing each sample with 50 μl of elution buffer and incubating these reactions for 5 minutes. Coomassie blue stained SDS PAGE gels of the assays were analysed by Densitometry using the program *ImageJ*. Normalization of the integrated peak areas of the gel bands was carried out as described above. The Vti1b band was chosen as a good measure for the amount of formed SNARE complex in Supp. Figure 7 since it is well separated from all other protein bands and stains strongly with Coomassie giving a high signal to noise ratio if compared to syntaxin7 and syntaxin8. The normalized intensities of the Vti1b bands at each time point in each of the three reactions were expressed as a ratio of the value for the normalized Vti1B band at t=4h 10min in the reconstitution reaction in the absence of Varp. These experiments showed that the effect of adding M684D Y687S Varp was the same as adding no Varp, demonstrating that M684D Y687S Varp does not bind to VAMP7.

In the case of the experiments described in Figure 6 and in Supp. Figure 8 the syntaxin7 and syntaxin8 bands were quantified together since in the assays using GST-VAMP7 SNARE motif as bait neither a reliable analysis of the Vti1B band was possible nor one of the syntaxin7 and 8 bands individually for technical reasons. For the assays using GST-VAMP7 CD in combination with Varp (658-921)-His_6 wt and Varp (658-921)-His_6 M684D Y687S the normalized intensities of the combined syntaxin7 and 8 bands of three independent experiments were averaged for each time point. These values were expressed as a ratio of the mean of the normalized syntaxin7 and 8 at time point t=24h 10min in the assay using Varp (658-921)-His_6 M684D Y687S. In the case of the assays using GST-VAMP7 SNARE motif the normalized values of the combined syntaxin7 and 8 bands were expressed as ratio of the normalized syntaxin7 and 8 bands at time point t=24h 10min in the respective experiment. These data agree with those of the shorter time course in that the presence of wt Varp slows down the rate of SNARE complex formation on full length VAMP7 by approximately 3.3 fold as compared to the situation in which the non-binding M684D Y687S Varp mutant was added. The rate of complex formation on the SNARE motif only of VAMP7 (i.e. lacking its longin domain) was approximately 20 times faster than that on the full length VAMP7.

For the assay investigating the competition between Vamp8 and Vamp7 (figure 7) the SNARE complex reconstitution was carried out in a similar manner to the assays described above but with the following additions. In the case of lanes "1xVAMP7" and "1xVAMP8" the molar ratio of GST-Vti1b–syntaxin7–syntaxin8–R-SNARE present was 1:4:4:4 whereas in lanes "VAMP7CD:VAMP8 10:1", "Varp:VAMP7CD:VAMP8 10:10:1" and "Varp:VAMP7CD:VAMP8 100:10:1" the ratio of GST-Vti1b–syntaxin7–syntaxin8–VAMP8 or VAMP7 was 1:4:4:4:40. Varp (658-921)-His_6 was added in molar ratios of 40:1 with respect to GST-Vti1b in the case of lane "Varp:VAMP7CD:VAMP8 10:10:1" and 400:1 with respect to GST-Vti1b in the case of lane "Varp:VAMP7CD:VAMP8 100:10:1". Including the pull down the reactions were incubated for 2.5 h and then stopped by washing off excessive, free protein.

Immunofluorescent confocal microscopy examining colocalization of Varp-HA and marker proteins.

NRK cells stably expressing Varp-HA were created using the pLXIN retroviral system (Clontech). Infectious virus particles were prepared by transfecting the Phoenix packaging cell line (gift of Andrew Peden) with pLXIN-Varp-HA. Virus containing media was filtered, supplemented with polybrene (5μg/mL) and placed on adherent NRK cells. Virally transduced cells were selected using Geneticin (Invitrogen) at 0.5mg ml^{-1} in complete media to generate a population of stably expressing cells. For immunofluorescence, stable cells

seeded on glass coverslips were rinsed with PBS then fixed with 3.7% paraformaldehyde in PBS for 20 minutes. Cells were rinsed 2x in TBS with 0.1% Tween-20 (TBS-T) then permeabilized by incubation with 0.1% Triton X-100 in TBS-T for 20 minutes. Cells were again rinsed 2x in TBS-T then incubated with blocking solution (5% non-fat dry milk powder in TBS-T) for 1 hour. Cells were incubated with primary antibody diluted in blocking solution for 1 hour, washed 3x with blocking solution, then incubated with fluorescently conjugated secondary antibodies (Invitrogen) diluted in blocking solution for 45 minutes. Cells were extensively washed with TBS-T, rinsed with ddH_2O and coverslips were mounted on glass slides using Prolong Gold Anti-Fade Reagent (Invitrogen). Single confocal sections and Z-series confocal images were captured using a Zeiss LSM-710 microscope (Carl Zeiss). The degree of colocalistionof Varp-HA and each individual marker protein was expressed as a Pearson R coefficient determined using Carl Zeiss Zen image analysis software

siRNA mediated knock-down in NRK cells

Endogenous Varp and Rab32 were knocked-down in wild-type NRK cells using siRNA oligo-nucleotides at 100nM transfected with DharmaFECT 2 (Dharmacon, Thermo) reagent according to the manufacturer's instructions. ON-TARGETplus SMARTpool oligo-nucleotides (4 individual oligos pooled together) were designed and synthesized by Dharmacon (Varp target sequence Rat ANKRD27, XM_341843, CAT#L-082171-01; Rab32 target sequence Rat RGD1559997, XM_344794, CAT#L-080263-01). Levels of knock-down were compared to cells transfected with a non-targeting control siRNA oligo-nucleotides at 100nM (Dharmacon, D-001810-01).

Supplementary references

1. Pryor, P.R., et al., *Molecular basis for the sorting of the SNARE VAMP7 into endocytic clathrin-coated vesicles by the ArfGAP Hrb.* Cell, 2008. **134**(5): p. 817-27.
2. Chiswell, B.P., et al., *The structural basis of integrin-linked kinase-PINCH interactions.* Proc Natl Acad Sci U S A, 2008. **105**(52): p. 20677-82.
3. Jacobs, M.D. and S.C. Harrison, *Structure of an IkappaBalpha/NF-kappaB complex.* Cell, 1998. **95**(6): p. 749-58.
4. Wilson, J.J. and R.A. Kovall, *Crystal structure of the CSL-Notch-Mastermind ternary complex bound to DNA.* Cell, 2006. **124**(5): p. 985-96.
5. Tong, S., et al., *Crystal structure of human osteoclast stimulating factor.* Proteins, 2009. **75**(1): p. 245-51.
6. Antonin, W., et al., *A SNARE complex mediating fusion of late endosomes defines conserved properties of SNARE structure and function.* EMBO J, 2000. **19**(23): p. 6453-64.
7. Bogdanovic, A., et al., *Syntaxin 7, syntaxin 8, Vti1 and VAMP7 (vesicle-associated membrane protein 7) form an active SNARE complex for early macropinocytic compartment fusion in Dictyostelium discoideum.* Biochem J, 2002. **368**(Pt 1): p. 29-39.
8. Pryor, P.R., et al., *Combinatorial SNARE complexes with VAMP7 or VAMP8 define different late endocytic fusion events.* EMBO Rep, 2004. **5**(6): p. 590-5.
9. Reaves, B.J., et al., *The effect of wortmannin on the localisation of lysosomal type I integral membrane glycoproteins suggests a role for phosphoinositide 3-kinase activity in regulating membrane traffic late in the endocytic pathway.* J Cell Sci, 1996. **109 (Pt 4)**: p. 749-62.
10. Linding, R., et al., *GlobPlot: Exploring protein sequences for globularity and disorder.* Nucleic Acids Res, 2003. **31**(13): p. 3701-8.
11. Deleage, G., C. Blanchet, and C. Geourjon, *Protein structure prediction. Implications for the biologist.* Biochimie, 1997. **79**(11): p. 681-6.